

## Dilepton production by bremsstrahlung of meson fields in nuclear collisions

I. N. Mishustin,<sup>1,2</sup> L. M. Satarov,<sup>1</sup> H. Stöcker,<sup>3</sup> and W. Greiner<sup>3</sup>

<sup>1</sup>The Kurchatov Institute, 123182 Moscow, Russia

<sup>2</sup>The Niels Bohr Institute, DK-2100 Copenhagen Ø, Denmark

<sup>3</sup>Institut für Theoretische Physik, J. W. Goethe Universität, D-60054 Frankfurt am Main, Germany

(Received 10 September 1997)

We study the bremsstrahlung of virtual  $\omega$  mesons due to the collective deceleration of nuclei at the initial stage of an ultrarelativistic heavy-ion collision. It is shown that electromagnetic decays of these mesons may give an important contribution to the observed yields of dileptons. Mass spectra of  $e^+e^-$  and  $\mu^+\mu^-$  pairs produced in central Au+Au collisions are calculated under some simplifying assumptions on the space-time variation of the baryonic current in a nuclear collision process. Comparison with the CERES data for 160A GeV Pb+Au collisions shows that the proposed mechanism gives a noticeable fraction of the observed  $e^+e^-$  pairs in the intermediate region of invariant masses. Sensitivity of the dilepton yield to the in-medium modification of masses and widths of vector mesons is demonstrated. [S0556-2813(98)01305-3]

PACS number(s): 25.75.Dw, 13.20.-v, 25.40.Ve

According to the relativistic mean-field model [1], strong time-dependent meson fields are generated in the course of a relativistic heavy-ion collision. Using the approach developed in papers on the pion [2] and photon [3] bremsstrahlung we suggested recently [4] a mechanism of particle production by the collective bremsstrahlung and decay of classical meson fields in relativistic heavy-ion collisions. The comparison with the observed data on pion multiplicity shows [5] that this mechanism may be important in central collisions of most heavy nuclei already at the SPS bombarding energy 160A GeV.

Within this mechanism the production of some particle(s)  $i$  is considered as a two-step process  $A_p + A_t \rightarrow \omega^* \rightarrow i + X$ . Here  $A_p(A_t)$  stands for the projectile (target) nucleus and  $\omega^*$  is a virtual vector meson.<sup>1</sup> The first step in the above reaction corresponds to the virtual bremsstrahlung process leading to the creation of an off-mass-shell vector meson. The second step is the superposition of all channels of the virtual meson decay with the particle  $i$  in the final state. Below we consider the production of virtual mesons in the coherent process caused by the collective deceleration of the projectile and target nuclei at the initial stage of the reaction. Preliminary results concerning the contribution of the above mechanism to the production of pions, real  $\omega$  mesons and dileptons are published in Ref. [5].

Below we focus mainly on the dilepton emission in central collisions of ultrarelativistic nuclei. The analysis of the dilepton production is interesting at least for two reasons. First, dileptons are highly penetrating particles and carry practically an undistorted information about their creation points. Second, a strong enhancement of the dilepton yield was observed recently in central 200A GeV S+Au [6], S+W [7], and 160A GeV Pb+Au [8] collisions. The analysis shows [9–11] that this enhancement can only partially be explained by the conventional mechanism of binary hadron

collisions, e.g., by  $\pi\pi \rightarrow \rho \rightarrow e^+e^-$  processes. According to Refs. [9,10] the experimental data can be reproduced assuming a strong reduction of the  $\rho$  meson mass in dense and hot nuclear matter. On the other hand, as argued in Ref. [11], the in-medium effect was probably overestimated in these calculations. Below we show that the enhanced dilepton yield may be explained, at least partly, by the contribution of the collective bremsstrahlung mechanism.

### I. FORMULATION OF THE MODEL

By analogy to the Walecka model we introduce the vector meson field  $\omega^\mu(x)$  coupled to the four-current  $J^\mu(x)$  of baryons participating in a heavy-ion collision at a given impact parameter  $b$ . The equation of motion determining the space-time evolution of  $\omega^\mu(x)$  can be written as ( $c = \hbar = 1$ )

$$(\partial^\nu \partial_\nu + m_\omega^2) \omega^\mu(x) = g_V J^\mu(x), \quad (1)$$

where  $g_V$  is the  $\omega NN$  coupling constant and  $m_\omega \simeq 783$  MeV is the omega meson mass. In the mean-field approximation  $\omega^\mu$  is considered as a purely classical field. From Eq. (1) one can see that excitation of propagating waves in the vacuum (the bremsstrahlung process) is possible if the Fourier transformed baryonic current

$$J^\mu(p) = \int d^4x J^\mu(x) e^{ipx} \quad (2)$$

is nonzero in the timelike region  $p^2 \sim m_\omega^2$ .

In the following we study the bremsstrahlung process in the lowest order approximation neglecting the back reaction and reabsorption of the emitted vector mesons, i.e., treating  $J^\mu$  as an external current. From Eq. (1) one can calculate the energy flux of the vector field at a large distance from the collision region [2]. Then this flux is expressed in terms of the distribution of field quanta, i.e.,  $\omega$  mesons. This leads to the following formulas for the momentum distribution of real  $\omega$  mesons emitted in a heavy-ion collision [12]:

<sup>1</sup>Here and below the virtual particles ( $\omega$ ,  $\rho$ , and  $\gamma$ ) are marked by a superscript asterisk.

$$E_\omega \frac{d^3 N_\omega}{d^3 p} = S(E_\omega, \mathbf{p}), \quad (3)$$

where  $E_\omega = \sqrt{m_\omega^2 + \mathbf{p}^2}$  and

$$S(p) = \frac{g_V^2}{16\pi^3} |J_\mu^*(p) J^\mu(p)| \quad (4)$$

is a source function. In our model the latter is fully determined by the collective motion of the projectile and target nucleons.

To take into account the off-mass-shell effects we characterize virtual  $\omega$  mesons by the mass  $M_\omega \equiv \sqrt{p^2}$  and total width  $\Gamma_{\omega^*}$ . The spectral function of virtual  $\omega$  mesons may be written as

$$\rho(M_\omega) = \frac{2}{\pi} \frac{M_\omega \Gamma_{\omega^*}}{(M_\omega^2 - m_\omega^2)^2 + m_\omega^2 \Gamma_{\omega^*}^2}. \quad (5)$$

To calculate the distribution of virtual mesons in their four-momenta  $p$  we use the formula [5]

$$\frac{d^4 N_{\omega^*}}{d^4 p} = \rho(M_\omega) S(p). \quad (6)$$

In the limit  $\Gamma_{\omega^*} \rightarrow 0$  one can replace  $\rho(M_\omega)$  by  $2\delta(M_\omega^2 - m_\omega^2)$ . In this case Eq. (6) becomes equivalent to the formula (3) for the spectrum of the on-mass-shell vector mesons. Below we study also how the dilepton production is changed when the pole position in the vector meson propagator is shifted due to the in-medium effects.

We consider the following channels of the virtual  $\omega$  decay, most important at invariant masses  $M_\omega \lesssim m_\omega$ :  $i = e^+e^-$ ,  $\mu^+\mu^-$ ,  $\pi^0\gamma$ ,  $\pi^0e^+e^-$ ,  $\pi^0\mu^+\mu^-$ ,  $\pi^+\pi^-$ ,  $\pi^+\pi^-\pi^0$ . The total width  $\Gamma_{\omega^*}$  is decomposed into the sum of partial decay widths  $\Gamma_{\omega^* \rightarrow i}$ :

$$\Gamma_{\omega^*} = \sum_i \Gamma_{\omega^* \rightarrow i}. \quad (7)$$

The distribution over the total four-momentum of particles in a given decay channel can be written as

$$\frac{d^4 N_{\omega^* \rightarrow i}}{d^4 p} = B_{\omega^* \rightarrow i} \frac{d^4 N_{\omega^*}}{d^4 p}, \quad (8)$$

where  $B_{\omega^* \rightarrow i} \equiv \Gamma_{\omega^* \rightarrow i} / \Gamma_{\omega^*}$  is the branching ratio of the  $i$ th decay channel. The latter is a function of the total invariant mass of the decay particles  $M = \sqrt{p^2} = M_\omega$ .

To calculate the four-current  $J^\mu(p)$  determining the source function  $S(p)$  we adopt the simple picture of a high-energy heavy-ion collision suggested in Ref. [4]. We consider collisions of identical nuclei ( $A_p = A_t = A$ ) at zero impact parameter. In the equal velocity frame the projectile and target nuclei initially move towards each other with velocities  $\pm v_0$  or rapidities  $\pm y_0$ , where  $v_0 = \tanh y_0 = (1 - 4m_N^2/s)^{1/2}$  and  $\sqrt{s}$  is the c.m. bombarding energy per nucleon. In the ‘‘frozen density’’ approximation [4] the internal compression and transverse motion of nuclear matter are disregarded at the early (interpenetration) stage of the reaction. Within this approximation the colliding nuclei

move as a whole along the beam axis with instantaneous velocities  $\dot{z}_p = -\dot{z}_t \equiv \dot{z}(t)$ . The projectile velocity  $\dot{z}(t)$  is a decreasing function of time, which we parametrize in the form [2]

$$\dot{z}(t) = v_f + \frac{v_0 - v_f}{1 + e^{t/\tau}}, \quad (9)$$

where  $\tau$  is the effective deceleration time and  $v_f$  is the final velocity of nuclei (at  $t \rightarrow +\infty$ ).

In this approximation the Fourier transform of the baryon current  $J^\mu(p)$  is totally determined by the projectile trajectory  $z(t)$  [4]:

$$\begin{aligned} J^0(p) &= \frac{P_\parallel}{p_0} J^3(p) \\ &= 2A \int_{-\infty}^{\infty} dt e^{ip_0 t} \cos[p_\parallel z(t)] F(\sqrt{\mathbf{p}_T^2 + p_\parallel^2} [1 - \dot{z}^2(t)]), \end{aligned} \quad (10)$$

where  $p_\parallel$  and  $\mathbf{p}_T$  are, respectively, the longitudinal and transverse components of the three-momentum  $\mathbf{p}$  and  $F(q)$  is the density form factor of the initial nuclei

$$F(q) \equiv \frac{1}{A} \int d^3 r \rho(r) e^{-i\mathbf{q} \cdot \mathbf{r}} = \frac{4\pi}{Aq} \int_0^\infty r dr \rho(r) \sin qr. \quad (11)$$

The time integrals in Eq. (10) were calculated numerically assuming the Woods-Saxon distribution of the nuclear density  $\rho(r)$ .

In this work we choose the same coupling constant  $g_V = 13.78$  and stopping parameters  $\tau$ ,  $v_f$  as in Ref. [4]. In particular, it is assumed that  $\tau$  equals one half of the nuclear passage time

$$\tau = \frac{R}{\sinh y_0}, \quad (12)$$

where  $R$  is the geometrical radius of initial nuclei,  $R = r_0 A^{1/3}$  with  $r_0 = 1.12$  fm. Instead of  $v_f$  it is more convenient to introduce the c.m. rapidity loss  $\delta y$  defined by the relation

$$v_f = \tanh(y_0 - \delta y). \quad (13)$$

For central Au+Au collisions we assume the energy-independent value [13]  $\delta y = 2.4$  for  $\sqrt{s} > 10$  GeV and the full stopping ( $\delta y = y_0$ ) for lower bombarding energies.

## II. DIFFERENT CHANNELS OF VIRTUAL MESON DECAY AND DILEPTON PRODUCTION

Similarly to Ref. [14] we assume that the ‘‘direct’’ decays of  $\omega$  mesons into dileptons,  $\omega^* \rightarrow l^+ l^-$ , proceed via the intermediate emission and decay of virtual photons  $\gamma^*$ . In the following the explicit formulas are presented for the  $e^+e^-$  production only. The corresponding expressions for dimuons are obtained by replacing the lepton masses and decay widths. The matrix element of the process  $\omega^* \rightarrow e^+e^-$  is proportional to the  $\omega$  meson polarization vector  $\xi_\mu$ , the lep-

ton current  $\bar{v}_+ \gamma^\mu u_-$ , and the photon propagator  $\propto k^{-2}$ , where  $k = p_+ + p_-$  is the total four-momentum of the lepton pair. The calculation of the partial decay width gives the result [14]

$$\Gamma_{\omega^* \rightarrow ee}(M) \propto M^{-4} \Gamma_{\gamma^* \rightarrow ee}. \quad (14)$$

Here  $M = \sqrt{k^2}$  is the dilepton invariant mass (in the direct channel  $M = M_\omega$ ) and  $\Gamma_{\gamma^* \rightarrow ee}$  is the partial width of a virtual photon

$$\Gamma_{\gamma^* \rightarrow ee} = \frac{\alpha\beta}{2} \left(1 - \frac{\beta^2}{3}\right) M \Theta(M - 2m_e), \quad (15)$$

where  $\alpha = e^2/\hbar c$ ,  $\Theta(x) \equiv \frac{1}{2}(1 + \text{sgn } x)$ ,  $m_e$  is the electron mass, and

$$\beta = \sqrt{1 - \frac{4m_e^2}{M^2}}. \quad (16)$$

The proportionality coefficient in Eq. (14) is determined from the condition  $B_{\omega^* \rightarrow ee}(m_\omega) = B_{ee}$ , where  $B_{ee} = 7.1 \times 10^{-5}$  is the observed probability of the  $\omega \rightarrow ee$  decay [15].

We take into account also the three-particle ‘‘Dalitz’’ decays  $\omega^* \rightarrow \pi^0 e^+ e^-$ . At fixed values of  $M$  and  $M_\omega$  the components of the total dilepton four-momentum  $k$  in the  $\omega$  rest frame can be found by using the expressions

$$k_0 = \sqrt{\mathbf{k}^2 + M^2} = \frac{M^2 + M_\omega^2 - m_\pi^2}{2M_\omega}, \quad (17)$$

where  $m_\pi = 0.14$  GeV is the pion mass. The corresponding partial width can be calculated assuming that the Dalitz decay is the two-step process  $\omega^* \rightarrow \pi \gamma^* \rightarrow \pi ee$ . Generalizing the results of [16] to the case of virtual  $\omega$ 's we obtain the following expression for the differential width of the Dalitz decay:

$$\frac{d\Gamma_{\omega^* \rightarrow \pi ee}}{dM} = \frac{2}{\pi M^2} \Gamma_{\omega^* \rightarrow \pi \gamma^*} \Gamma_{\gamma^* \rightarrow ee}. \quad (18)$$

The  $\omega^* \rightarrow \pi \gamma^*$  decay width is proportional to the electromagnetic form factor squared  $F_{\omega\pi}^2$ :

$$\Gamma_{\omega^* \rightarrow \pi \gamma^*} \propto F_{\omega\pi}^2 |\mathbf{k}|^3 \Theta(M_\omega - M - m_\pi), \quad (19)$$

where  $|\mathbf{k}|$  is determined from Eq. (17). The coefficient of proportionality may be found by considering the limiting case  $M_\omega \rightarrow m_\omega$ ,  $M \rightarrow 0$ , when the left-hand side of Eq. (19) coincides with the observed width of the  $\omega \rightarrow \pi \gamma$  decay. As shown in [16] the experimental data for  $F_{\omega\pi}$  are well reproduced within the vector meson dominance model [17]. Assuming that this model is valid also for decays of virtual  $\omega$ 's we have

$$F_{\omega\pi}^2 = \frac{m_\rho^2(m_\rho^2 + \Gamma_\rho^2)}{(M^2 - m_\rho^2)^2 + m_\rho^2 \Gamma_\rho^2}, \quad (20)$$

where  $m_\rho$  and  $\Gamma_\rho$  are the mass and total width of the  $\rho$  meson. Unless otherwise stated, Eq. (20) is used with the parametrization  $\Gamma_\rho = \Gamma_\rho(M)$  suggested in Ref. [14] and the free  $\rho$  meson mass ( $m_\rho = m_{\rho^0} \approx 0.77$  GeV).

In the softest region of invariant masses,  $M < m_\pi$ , the channels  $\omega^* \rightarrow 3\pi$ ,  $\omega^* \rightarrow \pi \gamma$  with the subsequent decay  $\pi^0 \rightarrow e^+ e^- \gamma$  become important. However, we do not consider the contribution of these processes for the following reasons. First, the corresponding mass region is strongly populated by decays of  $\pi^0$  mesons, produced in incoherent hadron-hadron collisions. Also, this region is not interesting from the viewpoint of dilepton enhancement observed by the CERES Collaboration at  $M > 2m_\pi$  [6,8]. The acceptance cuts used in these experiments strongly suppress the contribution of  $\pi^0$  decays.

To calculate the total width of virtual  $\omega$ 's one should know the partial widths of nonelectromagnetic decay channels. In the considered region of masses  $M_\omega \lesssim 1$  GeV we take into account the decays with two and three pions in the final state. Assuming that the  $\omega^* \rightarrow 2\pi$  matrix element is proportional to the product of the  $\omega$  meson polarization vector and the difference of the pion four-momenta, we get

$$\Gamma_{\omega^* \rightarrow 2\pi}(M_\omega) \propto M_\omega^{-2} (M_\omega^2 - 4m_\pi^2)^{3/2} \Theta(M_\omega - 2m_\pi). \quad (21)$$

The proportionality coefficient is taken from the condition  $B_{\omega^* \rightarrow 2\pi}(m_\omega) = B_{2\pi} = 0.022$  [15]. The  $\omega^* \rightarrow 3\pi$  partial width is calculated assuming that it is proportional to the three-pion phase space volume allowed by the kinematics [12]

$$\Gamma_{\omega^* \rightarrow 3\pi}(M_\omega) \propto \Phi_{3\pi}(M_\omega) \Theta(M_\omega - 3m_\pi), \quad (22)$$

with the coefficient determined from the relation  $B_{\omega^* \rightarrow 3\pi}(m_\omega) = B_{3\pi} = 0.89$  [15].

The mass distribution of  $e^+ e^-$  pairs produced by the bremsstrahlung mechanism can be written as a convolution of the virtual  $\omega$  meson spectrum and the differential branching of the  $\omega^* \rightarrow eeX$  decay [ $X$  denotes any particle(s) emitted together with the lepton pair]:

$$\frac{dN_{ee}}{dM} = \int d^4 p_\omega \frac{d^4 N_{\omega^*}}{d^4 p_\omega} \frac{dB_{\omega^* \rightarrow eeX}}{dM}. \quad (23)$$

Taking into account only the direct and Dalitz decays, the dilepton mass distribution can be represented as

$$\frac{dN_{ee}}{dM} = B_{\omega^* \rightarrow ee} \frac{dN_{\omega^*}}{dM} + \int_{M+m_\pi}^{\infty} dM_\omega \frac{dN_{\omega^*}}{dM_\omega} \frac{dB_{\omega^* \rightarrow ee\pi}}{dM}. \quad (24)$$

The first (direct) term is obtained by using the relation  $dB_{\omega^* \rightarrow ee}/dM = B_{\omega^* \rightarrow ee} \delta(M - M_\omega)$  and performing the explicit integration over  $M_\omega$ .

To compare the model predictions with experimental data one should take into account the various acceptance cuts used in different experiments. This severely complicates the calculations: in general one should know the differential branching  $d^6 B_{\omega^* \rightarrow eeX}/d^3 p_+ d^3 p_-$  which describes the probability of the  $\omega$  meson decay into the lepton pair with the positron and electron three-momenta  $\mathbf{p}_+$  and  $\mathbf{p}_-$ , respectively. To calculate the acceptance-weighted mass distribution one should replace  $dB_{\omega^* \rightarrow eeX}/dM$  in Eq. (23) by

$$\frac{dB_{\omega^* \rightarrow eeX}^{(A)}}{dM} = \int d^3p_+ d^3p_- \mathcal{A} \frac{d^6 B_{\omega^* \rightarrow eeX}}{d^3p_+ d^3p_-} \delta(M - \sqrt{k^2}). \quad (25)$$

The weight function  $\mathcal{A}$  equals one (zero) if  $\mathbf{p}_\pm$  are inside (outside) the kinematical volume covered in a given experiment. In numerical calculations presented in the next section we use for  $e^+e^-$  pairs the acceptance cuts of the CERES experiment [8]

$$p_{T\pm} > 0.175 \text{ GeV}/c, \quad 2.1 < \eta_\pm < 2.65, \quad \theta_{ee} > 0.035. \quad (26)$$

Here  $p_{T\pm}$  and  $\eta_\pm$  are the transverse momenta and pseudo-rapidities of leptons and  $\theta_{ee}$  is their relative emission angle in the lab frame.

At given  $M$  and  $M_\omega$  the components of the vectors  $\mathbf{p}_\pm$  are fixed by the angular variables  $\Omega = (\theta, \phi)$  and  $\tilde{\Omega} = (\tilde{\theta}, \tilde{\phi})$ , where  $\Omega$  denotes spherical angles of  $\mathbf{k}$  with respect to the  $\omega$  meson three-momentum (in its rest frame) and  $\tilde{\Omega}$  stands for the positron emission angles with respect to  $\mathbf{k}$  (in the pair rest frame). By using these variables one can rewrite Eq. (25) as follows:

$$\frac{dB_{\omega^* \rightarrow eeX}^{(A)}}{dM} = \frac{dB_{\omega^* \rightarrow eeX}}{dM} \int d\Omega \int d\tilde{\Omega} \frac{dW_{\omega^* \rightarrow eeX}}{d\Omega d\tilde{\Omega}} \mathcal{A}, \quad (27)$$

where  $dW_{\omega^* \rightarrow eeX}/d\Omega d\tilde{\Omega}$  is the angular distribution of the  $\omega^* \rightarrow eeX$  decay normalized to unity.

In our case the usual procedure of calculating the direct and Dalitz contributions by simple averaging over all polarizations of decaying  $\omega$  mesons is not correct. Indeed, as seen from Eq. (1), the polarization vector of a virtual vector meson  $\xi_\mu$  is proportional to  $J_\mu(p)$  where  $p$  is the meson four-momentum. In the  $\omega$  meson rest frame  $\xi_\mu = (0, \boldsymbol{\xi})$ , where  $\boldsymbol{\xi}$  is a vector parallel to the direction of  $\mathbf{p}$ . Proceeding from the  $\omega^* \rightarrow ee$  matrix element (see above) we get the following relation for the direct part of the angular distribution:

$$\frac{dW_{\omega^* \rightarrow ee}}{d\Omega d\tilde{\Omega}} = C_{\text{dir}} (1 - \beta^2 \cos^2 \tilde{\theta}) \delta(\Omega), \quad (28)$$

where  $C_{\text{dir}}$  is the normalization constant. The anisotropy of the lepton angular distribution in the rest frame of the  $\omega$  meson is a consequence of its polarization.

The Dalitz part of the dilepton distribution is calculated assuming [14,16] that the  $\omega^* \rightarrow ee\pi$  matrix element is proportional to  $\epsilon_{\mu\nu\sigma} \delta \xi^\mu p^\nu k^\sigma (\bar{v}_+ \gamma^\delta u_-)$ . The direct calculation gives

$$\frac{dW_{\omega^* \rightarrow ee\pi}}{d\Omega d\tilde{\Omega}} = C_{\text{dal}} \sin^2 \theta [1 - \beta^2 \sin^2 \tilde{\theta} \sin^2(\tilde{\phi} - \phi)], \quad (29)$$

where  $C_{\text{dal}}$  is found from the normalization condition. The averaging over the  $\omega$  meson polarizations is equivalent to the averaging over  $\Omega$ . As a result we obtain the distribution over  $\tilde{\Omega}$  obtained earlier in Ref. [18].

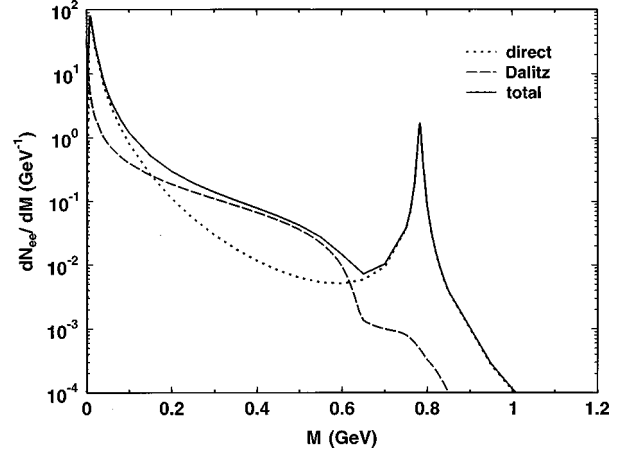


FIG. 1. Mass spectrum of  $e^+e^-$  pairs produced by the collective bremsstrahlung mechanism in central 160A GeV Au+Au collisions. Contributions of the direct ( $\omega^* \rightarrow ee$ ) and Dalitz ( $\omega^* \rightarrow \pi ee$ ) decay channels are shown by dotted and dashed lines, respectively.

### III. RESULTS

Let us now discuss the results of numerical calculations obtained within the model described above. One should bear in mind that the model assumes a rather simplified space-time evolution, in particular the collective projectile-target deceleration (see the discussion in Ref. [4]). Therefore, the model in its present form can be used for a qualitative analysis only.

Figure 1 shows the dilepton mass spectrum in central ( $b=0$ ) 160A GeV Au+Au collisions. One can see that the mass distribution of dileptons produced by the virtual  $\omega$  decays is quite different from that predicted by the conventional hadronic sources. In particular, the low and intermediate mass region is strongly enhanced. This is explained by the copious production of “soft” virtual  $\omega$ 's by the bremsstrahlung mechanism. The contribution of direct  $\omega$  decays is peaked at very small invariant masses as well as at the pole position of the  $\omega$  propagator  $M = m_\omega$ . The Dalitz contribution is most important in the intermediate region of dilepton masses,  $0.2 \text{ GeV} \leq M \leq 0.6 \text{ GeV}$ . A similar behavior is predicted for the dimuon spectrum,<sup>2</sup> Fig. 2. The main difference here is the much higher mass threshold at  $M = 2m_\mu$ .

In Fig. 3 we compare the model predictions for the same reaction, but at different bombarding energies  $\sqrt{s} = 17.43A \text{ GeV}$  (SPS) and 200A GeV (RHIC). We have also calculated the dilepton spectra at the LHC energy  $\sqrt{s} = 6.3A \text{ TeV}$  but the corresponding results practically coincide with the model prediction for the RHIC energy. Such a behavior follows from the energy independence of the stopping parameter  $\delta y$ , assumed at high  $\sqrt{s}$  (see Sec. I). As a consequence, the phase-space distribution of primordial  $\omega$  mesons, produced by the bremsstrahlung mechanism, saturates with raising bombarding energy [4].

Due to the experimental acceptance cuts and a poor mass

<sup>2</sup>Since the branching ratio of the direct decay  $\omega \rightarrow \mu^+ \mu^-$  is not known experimentally [15] we assume that it is equal to  $B(\omega \rightarrow e^+ e^-)$ .

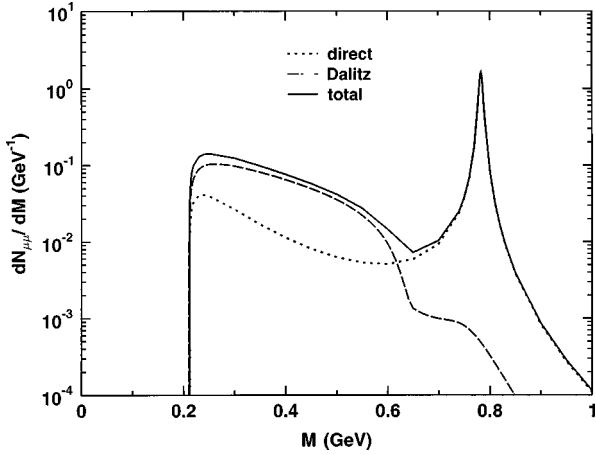


FIG. 2. The same as in Fig. 1, but for the spectrum of  $\mu^+\mu^-$  pairs.

resolution the dilepton mass distributions receive significant distortions as compared to those presented in Figs. 1–3. In Fig. 4 we show the dilepton mass spectrum for central 160A GeV Au+Au collisions. The CERES acceptance cuts and mass resolution are included in this calculation. The double differential spectrum  $d^2N_{ee}/dM d\eta$  is obtained by dividing the acceptance-weighted mass distribution, Eq. (24), by the width of the CERES pseudorapidity window. In calculating the acceptance weight  $\mathcal{A}$  entering Eq. (27) we have neglected the transverse momenta of primordial  $\omega$  mesons (see Ref. [4]). At the same figure we show separately the contributions of direct and Dalitz decays of  $\omega$  mesons. Note that the original spectrum (without mass resolution corrections) of  $e^+e^-$  pairs has a strong peak at  $M \approx m_\omega$ . This peak originates from the direct  $\omega$  meson decays. The steplike behavior of the direct contribution at  $M \approx 0.35$  GeV appears due to the CERES cut at small transverse momenta,  $p_{T\pm} > p_{\min} = 0.175$  GeV/c. Indeed, in the limit  $p_{T\omega} = 0$  the minimal invariant mass of “direct” pairs is  $2\sqrt{m_e^2 + p_{\min}^2} \approx 0.35$  GeV. Taking into account nonzero components of  $\mathbf{p}_{T\omega}$  will result in a certain smoothing of the above-mentioned jump in the dilepton mass distribution.

As one can see from Fig. 4, the bremsstrahlung mechanism gives a significant contribution to the dilepton produc-

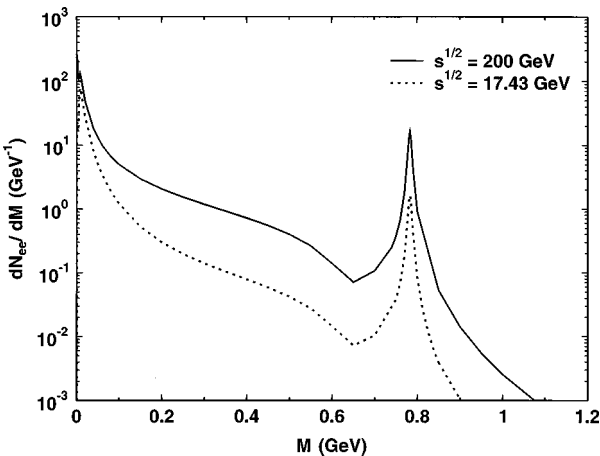


FIG. 3. Comparison of  $e^+e^-$  yields in central Au+Au collisions at the SPS and RHIC bombarding energies.

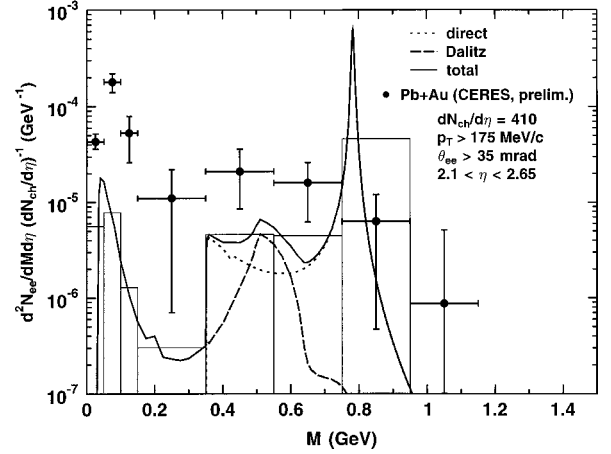


FIG. 4. Mass spectrum of  $e^+e^-$  pairs produced by the collective bremsstrahlung mechanism in central 160A GeV Au+Au collisions. The grey histogram (solid line) shows the model results with (without) inclusion of experimental mass resolution. The dotted (dashed) line shows the contribution of direct (Dalitz)  $\omega$  meson decays. Preliminary experimental data for central Pb+Au collisions [8] are shown by solid dots.

tion in the intermediate mass region. However, the bremsstrahlung contribution alone is not sufficient to explain the dilepton yield observed in central 160A GeV Pb+Au collisions. In the most interesting region of masses  $M \approx 0.4$ – $0.6$  GeV the data are still underestimated by a factor of about 3.

Simple estimates show that this discrepancy cannot be removed by taking into account the excitation and decays of virtual  $\rho$  mesons disregarded in the present calculation. Indeed, the collective bremsstrahlung of  $\rho$  mesons may be treated analogously to the  $\omega$  meson case. The equation of motion for the  $\rho^0$  field may be written as [1]

$$(\partial^\nu \partial_\nu + m_\rho^2) \rho_\mu^0 = g_\rho J_\mu^0. \quad (30)$$

Here  $g_\rho$  is the  $\rho NN$  coupling constant and  $J_\mu^0 = 1/2 \bar{\psi} \tau^3 \gamma_\mu \psi$  is the zero component of the isovector baryonic current. To estimate  $J_\mu^0$  we assume that local values of the neutron to proton ratio are not changed significantly in the course of a heavy-ion collision. In this approximation  $J_\mu^0 \approx \chi J_\mu$ , where  $\chi = 1/2 - Z/A$  is the isospin asymmetry factor of the colliding nuclei, determined by their charge ( $Z$ ) and mass ( $A$ ) numbers. The spectrum of virtual  $\rho$  mesons produced by the bremsstrahlung mechanism is given by Eqs. (4)–(6) with the replacement  $g_V J_\mu, m_\omega, \Gamma_{\omega^*} \rightarrow g_\rho J_\mu, m_\rho, \Gamma_{\rho^*}$ . Using the formulas of Sec. II and taking into account only direct channels of vector meson decays one may estimate the ratio of integrated yields of dileptons produced by bremsstrahlung of  $\rho$  and  $\omega$  mesons as

$$\frac{N_{AA \rightarrow \rho^0 \rightarrow e^+e^-}}{N_{AA \rightarrow \omega^* \rightarrow e^+e^-}} \approx \left( \frac{g_\rho}{g_V} \chi \right)^2 \frac{B_{\rho^0 \rightarrow e^+e^-}}{B_{\omega \rightarrow e^+e^-}}. \quad (31)$$

Substituting  $g_\rho = 8.08$  [19] we obtain that in the case of a central Au+Au collision this ratio is of the order of  $3 \times 10^{-3}$ . The relative contribution of  $\rho$  mesons becomes even smaller for lighter nuclei.

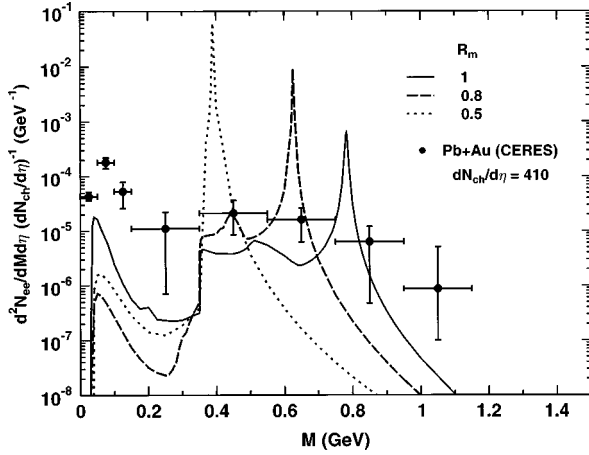


FIG. 5. Comparison of  $e^+e^-$  spectra in central 160A GeV Au+Au collisions for different values of the meson mass reduction factor  $R_m$ . Experimental data for central Pb+Au collisions are taken from Ref. [8].

Of course, in addition to the collective bremsstrahlung mechanism the usual, incoherent, sources of dilepton production (e.g., the  $\pi\pi \rightarrow ee$  and  $\pi \rightarrow ee\gamma$  processes) also give a noticeable contribution. According to Refs. [9–11] the dynamical models incorporating only these incoherent hadronic sources may easily explain the low mass dilepton yields in S+Au and Pb+Au collisions at the SPS energies. On the other hand, these models significantly underestimate the observed data in the intermediate mass region. As argued in Refs. [9,10] the agreement with experimental data can be achieved if one assumes a strong reduction of the vector meson masses in dense nuclear matter.

To check the sensitivity of our model to the in-medium modification of the vector mesons, in Fig. 5 we compare the dilepton mass distributions calculated for different values of the  $\rho$  and  $\omega$  masses. To diminish the number of model parameters we take the same mass reduction factor for  $\rho$  and  $\omega$  mesons:  $m_\rho/m_{\rho 0} = m_\omega/m_{\omega 0} \equiv R_m$ . One can see that the dilepton yields are rather sensitive to  $R_m$ . A relatively small, 20%, reduction of the meson masses raises the dilepton yield at  $M \sim 0.5$  GeV by a factor of about 2. On the other hand, the model calculation with fixed  $R_m$  predicts too high peaks in mass distributions. One should bear in mind that these calculations provide only a rough estimate of the possible effect since in an actual nuclear collision the mass shifts should be time and space dependent. Therefore, the observed spectrum will be a superposition of contributions with different  $R_m$ . As a result, the peak of direct dileptons will be smoothed out in the integrated distribution.

As shown in Refs. [20,21], the  $\omega$  meson width may increase significantly in a dense nuclear matter. At baryonic densities of the order of the normal nuclear density, the width may exceed the vacuum value by a large factor  $\lambda \sim 10$ . On the other hand, the  $\omega$  meson mass is predicted to lower only slightly in this case. To estimate the effects of the in-medium broadening of virtual  $\omega$  mesons, we have performed the calculation where the partial decay widths were scaled by the same amplification factor  $\lambda$ , independent of  $M_\omega$ . The calculation shows that this broadening affects mainly the direct component of the dilepton yield. As seen

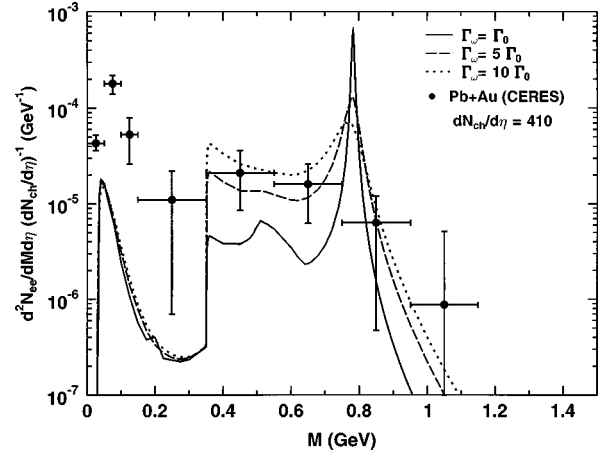


FIG. 6. The same as in Fig. 5 but for different choices of the virtual  $\omega$  width in units of the vacuum width  $\Gamma_0 = 8.4$  MeV.

from Fig. 6, the yield in the region  $0.35 \text{ GeV} \lesssim M \lesssim 0.7$  GeV is strongly enhanced for  $\lambda \gtrsim 5$ .

Additional experiments are necessary to establish the role played by the collective bremsstrahlung mechanism. It would be very useful to measure the distributions over total transverse momentum  $p_T$  and rapidity  $y$  of a dilepton pair. These distributions have two characteristic features. First, as follows from Eq. (10), the  $p_T$  distribution should be relatively soft, due to the cutoff  $p_T \lesssim \hbar/R$  imposed by the nuclear form factor. Second, as shown in Ref. [22], the rapidity distribution should have a dip at  $y_{c.m.} = 0$ , due to the cancellation of projectile and target currents. This dip is especially pronounced at higher invariant masses when the Dalitz contribution is relatively small.

#### IV. SUMMARY

In conclusion, we have shown that the collective bremsstrahlung of the vector meson field can provide an important source of dilepton production in high-energy heavy-ion collisions. This mechanism may be responsible, at least partly, for the enhanced yield of dileptons observed in central nuclear collisions at the SPS bombarding energies. It has been demonstrated that the coherent dilepton production is sensitive to the in-medium modification of vector meson masses and widths. Obviously, these effects should be studied in more detail in microscopic models.

In future studies it will be necessary to implement a more realistic dynamical picture of a heavy-ion collision by using either the fluid-dynamical or kinetic approach. In this way one can take into account the flow and compression effects disregarded in the present model. Decoherence effects due to the stochastic scatterings and finite formation times of hadrons should be studied. Also the formalism should be generalized to study bremsstrahlung effects in a situation when masses and widths of vector mesons are space and time dependent. To extend the calculations to collider energies,  $\sqrt{s} \gtrsim 200$  GeV, the model should be reformulated on the quark-gluon level.

## ACKNOWLEDGMENTS

The authors thank J. P. Bondorf and L. A. Winckelmann for useful discussions and J. Stachel and Th. Ullrich for providing valuable information on CERES data. This work was supported in part by the Carlsberg Foundation (Denmark)

and EU-INTAS Grant No. 94-3405. We acknowledge also the financial support from GSI, BMFT, and DFG. Two of us (I.N.M., L.M.S.) thank the Institute for Theoretical Physics, University of Frankfurt am Main, and the Niels Bohr Institute, University of Copenhagen, for the kind hospitality and financial support.

- 
- [1] B. D. Serot and J. D. Walecka, *Adv. Nucl. Phys.* **16**, 1 (1985).  
 [2] D. Vasak, H. Stöcker, B. Müller, and W. Greiner, *Phys. Lett.* **93B**, 243 (1980); D. Vasak, B. Müller, and W. Greiner, *Phys. Scr.* **22**, 25 (1980).  
 [3] T. Lippert, U. Becker, N. Grün, W. Scheid, and G. Soff, *Phys. Lett. B* **207**, 366 (1988).  
 [4] I. N. Mishustin, L. M. Satarov, H. Stöcker, and W. Greiner, *Phys. Rev. C* **52**, 3315 (1995).  
 [5] I. N. Mishustin, L. M. Satarov, and H. Stöcker, in *Proceedings of the International Conference on Nuclear Physics at the Turn of the Millenium*, Wilderness, South Africa, 1996, edited by H. Stöcker, A. Gallman, and J. H. Hamilton (World Scientific, Singapore, 1997), p. 522; I. N. Mishustin, L. M. Satarov, H. Stöcker, and W. Greiner, hep-ph/9611295, 1996.  
 [6] G. Agakishiev *et al.*, CERES Collaboration, *Phys. Rev. Lett.* **75**, 1272 (1995).  
 [7] M. Masera for the HELIOS-3 Collaboration, *Nucl. Phys.* **A590**, 93c (1995).  
 [8] G. Agakishiev *et al.*, CERES Collaboration, *Nucl. Phys.* **A610**, 317c (1996).  
 [9] G. Q. Li, C. M. Ko, and G. E. Brown, *Phys. Rev. Lett.* **75**, 4007 (1995); C. M. Ko, G. Q. Li, G. E. Brown, and H. Sorge, *Nucl. Phys.* **A610**, 342c (1996).  
 [10] W. Cassing, W. Ehehalt, and C. M. Ko, *Phys. Lett. B* **363**, 35 (1995).  
 [11] L. A. Winckelmann *et al.*, *Nucl. Phys.* **A610**, 116c (1996).  
 [12] Yu. B. Ivanov, *Nucl. Phys.* **A495**, 633 (1989).  
 [13] Th. Schönfeld, H. Stöcker, W. Greiner, and H. Sorge, *Mod. Phys. Lett. A* **8**, 2631 (1993).  
 [14] P. Koch, *Z. Phys. C* **57**, 283 (1993).  
 [15] Particle Data Group, L. Montanet *et al.*, *Phys. Rev. D* **50**, 1173 (1994).  
 [16] L. G. Landberg, *Phys. Rep.* **128**, 301 (1985).  
 [17] J. J. Sakurai, *Currents and Mesons* (University of Chicago Press, Chicago, 1969).  
 [18] N. M. Kroll and W. Wada, *Phys. Rev.* **98**, 1355 (1955).  
 [19] C. J. Horowitz and B. D. Serot, *Nucl. Phys.* **A368**, 503 (1981).  
 [20] G. Wolf, B. Friman, and M. Soyer, nucl-th/9707055.  
 [21] F. Klingl, N. Kaiser, and W. Weise, *Nucl. Phys.* **A624**, 527 (1997).  
 [22] I. N. Mishustin, L. M. Satarov, H. Stöcker, and W. Greiner, *J. Phys. G* **24**, L17 (1998).